Orbital-free kinetic-energy density functionals with a density-dependent kernel

Yan Alexander Wang, Niranjan Govind, and Emily A. Carter
Department of Chemistry and Biochemistry, Box 951569, University of California, Los Angeles, California 90095-1569
(Received 26 May 1999; revised manuscript received 10 August 1999)

We report linear-response kinetic-energy density functionals, which show significant improvement over the Wang-Teter, Perrot, Smargiassi-Madden, Wang-Govind-Carter functionals, yet still maintain $\mathcal{O}(N \ln N)$ scaling. Numerical tests show that these functionals, which contain a double-density-dependent kernel, can reproduce the Kohn-Sham results almost exactly for several aluminum bulk phases. We further show that with a sensible choice of the uniform background density, energies of formation for the low-index aluminum surfaces, where the density variations are very large, can be reproduced to within reasonable accuracy.
[S0163-1829(99)01848-2]

I. BACKGROUND

Among all linear-scaling $\mathcal{O}(N)$ density-functional methods,[1–7] the orbital-free Hohenberg-Kohn scheme[2–8] is potentially the most attractive. Without any orbital dependence, the complication and cost associated with orbital manipulation, including orbital localization and orbital orthonormalization, are avoided. For metals, the orbital-free scheme is even more rewarding, because the need for Brillouin-zone (**k**-point) sampling[9] is completely eliminated. However, all these positive features come at a price: accurate, transferable orbital-free kinetic-energy density functionals do not, as yet, exist in our $\mathcal{O}(N)$ arsenal. We set our task toward surmounting this problem in this paper.

The Wang-Teter (WT), Perrot, Smargiassi-Madden (SM), Wang-Govind-Carter (WGC) kinetic-energy density functionals (KEDF's) can be conveniently written as[3–7]

$$T_s^{\{\alpha\}}[\rho]=\sum_\alpha T_s^\alpha[\rho]=T_{\mathrm{TF}}[\rho]+T_{\mathrm{vW}}[\rho]+\sum_\alpha \lambda_\alpha T_X^\alpha[\rho], \tag{1}$$

$$T_{\mathrm{TF}}[\rho]=\langle t_{\mathrm{TF}}(\mathbf{r})\rangle=C_{\mathrm{TF}}\langle\rho^{5/3}(\mathbf{r})\rangle, \tag{2}$$

$$T_{\mathrm{vW}}[\rho]=\langle t_{\mathrm{vW}}(\mathbf{r})\rangle=\frac{1}{8}\left\langle\frac{|\nabla\rho(\mathbf{r})|^2}{\rho(\mathbf{r})}\right\rangle, \tag{3}$$

$$T_X^\alpha[\rho]=C_{\mathrm{TF}}\langle\rho^\alpha(\mathbf{r})|w_\alpha(\mathbf{r}-\mathbf{r}')|\rho^\alpha(\mathbf{r}')\rangle. \tag{4}$$

Here, $T_{\mathrm{TF}}[\rho]$ is the Thomas-Fermi (TF) functional,[10] $C_{\mathrm{TF}}=\frac{3}{10}(3\pi^2)^{2/3}$, and $T_{\mathrm{vW}}[\rho]$ is the von Weizsäcker (vW) functional.[11] $\{\alpha\}$ are positive parameters which define $X=$Wang-Teter-Perrot[3,4] for $\alpha=\frac{5}{6}$, $X=$Perrot[4] for $\alpha=1$, $X=$SM[5,7] for $\alpha=\frac{1}{2}$, and $X=$WGC[6] for other choices of α. $\{\lambda_\alpha\}$ are the corresponding expansion weights that satisfy $\Sigma_\alpha\lambda_\alpha=1$.[6] The original WT, Perrot, and SM KEDF's only had one term in the sum in Eq. (1), and were generalized to have more terms recently.[6]

The specific form of Eq. (4) is chosen based on the following analysis. First, one can rewrite $T_{\mathrm{TF}}[\rho]$ and $T_{\mathrm{vW}}[\rho]$ in double-integration form[12]

$$T_{\mathrm{TF}}[\rho]=C_{\mathrm{TF}}\langle\rho^{5/6}(\mathbf{r})|\,\delta(\mathbf{r}-\mathbf{r}')|\rho^{5/6}(\mathbf{r}')\rangle, \tag{5}$$

$$T_{\mathrm{vW}}[\rho]=-\frac{1}{4}\langle\rho^{1/2}(\mathbf{r})|\,\delta(\mathbf{r}-\mathbf{r}')\nabla^2+\nabla^2\delta(\mathbf{r}-\mathbf{r}')|\rho^{1/2}(\mathbf{r}')\rangle. \tag{6}$$

It is well known that $T_{\mathrm{TF}}[\rho]$ is only exact at the free-electron gas limit and $T_{\mathrm{vW}}[\rho]$ is only exact for those systems that can be described by a single spatial orbital, i.e., the one- and two-electron ground-state systems.[13] Any realistic system that falls between these two extremes will have to be bridged somehow by a third term, which can also smoothly recover the two extreme cases if appropriate conditions are met. Eq. (4) is then a natural choice for this functional because it possesses the same form as Eqs. (5) and (6). Second, there is no reason to go beyond the double-integration form because the highest rank of the operators in the quantum mechanical Hamiltonian for isolated Coulomb systems is two. This simply means that for any second-rank operator of the form

$$\hat{O}=\sum_{i,j}\hat{o}_{ij}, \tag{7}$$

its expectation value can be described by the second-order reduced density matrix[14] Γ_2

$$\langle\Psi|\hat{O}|\Psi\rangle=\langle\hat{o}_{12}\Gamma_2\rangle, \tag{8}$$

where Ψ is the total normalized wave function. One step further, one instantly has

$$\langle\Psi|\hat{O}|\Psi\rangle=\left\langle\rho^\alpha(\mathbf{r})\left|\frac{\hat{o}_{12}\Gamma_2}{\rho^\alpha(\mathbf{r})\rho^\beta(\mathbf{r}')}\right|\rho^\beta(\mathbf{r}')\right\rangle, \tag{9}$$

where α and β are positive parameters. Aside from the explicit density-dependence in the kernel, Eq. (9) is clearly of the same form as Eq. (4) when $\alpha=\beta$. Third, a more detailed analysis based on Natural Variable arguments[15] reveals a deeper understanding about the mathematical structure of the kernel in Eq. (9). Historically, the KEDF's in Eq. (1) were designed solely on the grounds of point 1 above.[3–8] We intend in this paper to coherently take all three points into consideration.

To comply with the first point, the kernel $w_\alpha(\mathbf{r}-\mathbf{r}')$ is chosen such that each term in the sum in Eq. (1), T_s^α, satis-

fies the known exact linear response (LR) for a uniform Hartree electron gas without exchange,

$$\hat{F}\left(\left.\frac{\delta^2 T_s^{\alpha}[\rho]}{\delta\rho(\mathbf{r})\,\delta\rho(\mathbf{r}')}\right|_{\rho_0}\right)=-\frac{1}{\chi_{\mathrm{Lind}}}=\frac{\pi^2}{k_F}F(\eta), \tag{10}$$

$$F(\eta)=\left(\frac{1}{2}+\frac{1-\eta^2}{4\eta}\ln\left|\frac{1+\eta}{1-\eta}\right|\right)^{-1}, \tag{11}$$

where $\hat{F}$ denotes the Fourier transform, ρ_0 is the average electron density, χ_{Lind} is the Lindhard susceptibility function in reciprocal space,[16] $k_F=(3\pi^2\rho_0)^{1/3}$ is the Fermi wave vector, and $\eta=q/(2k_F)$ is a dimensionless momentum. In other words, $w_\alpha(\mathbf{r}-\mathbf{r}')$ can be expressed in reciprocal space as[4–7]

$$\hat{F}w_\alpha(\mathbf{r}-\mathbf{r}')=\tilde{w}_\alpha(\mathbf{q})=-\frac{\chi_{\mathrm{Lind}}^{-1}-\chi_{\mathrm{vW}}^{-1}-\chi_{\mathrm{TF}}^{-1}}{2\alpha^2 C_{\mathrm{TF}}\rho_0^{2(\alpha-1)}}=\frac{5G(\eta)}{9\alpha^2\rho_0^{2\alpha-5/3}}, \tag{12}$$

$$G(\eta)=F(\eta)-3\eta^2-1, \tag{13}$$

where $\chi_{\mathrm{TF}}=-(k_F/\pi^2)$ is the TF LR function and $\chi_{\mathrm{vW}}=\chi_{\mathrm{TF}}/(3\eta^2)$ is the vW LR function. To keep the exact LR intact for the total KEDF in Eq. (1), the expansion weights have to satisfy the normalization constraint $\Sigma_\alpha\lambda_\alpha=1$.[6]

II. FUNCTIONAL WITH A DENSITY-INDEPENDENT KERNEL

The previous discussion motivates the following more general trial KEDF:

$$T_s^{\alpha,\beta}[\rho]=T_{\mathrm{TF}}[\rho]+T_{\mathrm{vW}}[\rho]+T_Y^{\alpha,\beta}[\rho], \tag{14}$$

$$T_Y^{\alpha,\beta}[\rho]=C_{\mathrm{TF}}\langle\rho^\alpha(\mathbf{r})|w_{\alpha,\beta}(\mathbf{r}-\mathbf{r}')|\rho^\beta(\mathbf{r}')\rangle, \tag{15}$$

where α and β are positive parameters. By enforcing the exact LR as done in Eq. (10), we can express the kernel $w_{\alpha,\beta}(\mathbf{r}-\mathbf{r}')$ in reciprocal space as

$$\tilde{w}_{\alpha,\beta}(\mathbf{q})=-\frac{\chi_{\mathrm{Lind}}^{-1}-\chi_{\mathrm{vW}}^{-1}-\chi_{\mathrm{TF}}^{-1}}{2\alpha\beta C_{\mathrm{TF}}\rho_0^{\alpha+\beta-2}}=\frac{5G(\eta)}{9\alpha\beta\rho_0^{\alpha+\beta-5/3}}, \tag{16}$$

which is fully consistent with Eq. (12) when $\alpha=\beta$. Following the same procedure as given before,[6] one can arrive at equations similar to Eqs. (24) and (25) of Ref. 6. For slowly varying densities or the $q\to 0$ limit,

$$T_s^{\alpha,\beta}\to T_{\mathrm{TF}}+\frac{1}{9}\;T_{\mathrm{vW}}-\frac{8}{9}(\alpha+\beta-1)\langle\delta\sigma|t_{\mathrm{vW}}\rangle-\frac{4}{9}(\alpha+\beta-1)(\alpha+\beta-2)\langle\delta\sigma^2|t_{\mathrm{vW}}\rangle+\mathcal{O}(\delta\sigma^3) \tag{17}$$

and for rapidly varying densities or the $q\to\infty$ limit,

$$T_s^{\alpha,\beta}\to T_{\mathrm{vW}}+\left(1-\frac{8}{9\alpha\beta}\right)T_{\mathrm{TF}}-\frac{8}{9\alpha\beta}\left(\alpha+\beta-\frac{5}{3}\right)\langle\delta\sigma|t_{\mathrm{TF}}\rangle-\frac{4}{9\alpha\beta}\left(\alpha+\beta-\frac{5}{3}\right)\left(\alpha+\beta-\frac{8}{3}\right)\langle\delta\sigma^2|t_{\mathrm{TF}}\rangle+\mathcal{O}(\delta\sigma^3), \tag{18}$$

where $\delta\sigma=\rho(\mathbf{r})/\rho_0-1$. For the nearly free electron gas, $|\delta\sigma|\ll 1$.

Unlike the original KEDF's in Eq. (1), it is now possible for a single set of $\{\alpha,\beta\}$ to simultaneously remove all spurious $\delta\sigma$ terms from Eq. (18), and reduce it to the correct large-q limit[6] (CLQL): $T_{\mathrm{vW}}-\frac{3}{5}T_{\mathrm{TF}}$. Since the CLQL of T_s^α approximates χ_{Lind} well for most η values larger than 1, while the second-order conventional gradient expansion[17] (CGE) is only good for a small area close to $\eta=0$,[6] it is reasonable to focus our attention on eliminating all the spurious $\delta\sigma$ terms in Eq. (18). Thus, we simply require the solution of the following two equations:

$$1-\frac{8}{9\alpha\beta}=-\frac{3}{5}\;\text{ and }\;\alpha+\beta=\frac{5}{3}, \tag{19}$$

which is

$$\alpha,\beta=\frac{5}{6}\pm\frac{\sqrt{5}}{6}, \tag{20}$$

symmetrically displaced around $\frac{5}{6}$.

We note that the general KEDF in Eq. (14) has been suggested previously by Wang and Teter[3] with

$$\{\alpha,\beta\}=\left\{\frac{5}{6}\pm\frac{4\sqrt{2}-5}{6}\right\},$$

via a different approach.

III. FUNCTIONALS WITH A DOUBLE-DENSITY-DEPENDENT KERNEL

So far, we have only considered KEDF's without any density dependence in the kernels. We can of course introduce density-dependence into the kernels, in the same spirit as Chacón and co-workers.[8] Unfortunately, this comes at the expense of greatly complicating the derivation and making a straightforward numerical implementation computationally expensive, scaling quadratically with grid size.[8] Nonetheless, we will introduce a way around this problem in Sec. IV, and the scheme still scales as $\mathcal{O}(N\ln N)$.

Introducing two $\rho(\mathbf{r})$'s in the kernel of Eq. (14),[8,15] one has

$$T_s^{\alpha,\beta}[\rho]=T_{\mathrm{TF}}[\rho]+T_{\mathrm{vW}}[\rho]+T_Z^{\alpha,\beta}[\rho], \tag{21}$$

$$T_Z^{\alpha,\beta}[\rho]=C_{\mathrm{TF}}\langle\rho^\alpha(\mathbf{r})|w_{\alpha,\beta}[\xi_\gamma(\mathbf{r},\mathbf{r}'),\mathbf{r}-\mathbf{r}']|\rho^\beta(\mathbf{r}')\rangle, \tag{22}$$

$$\xi_\gamma(\mathbf{r},\mathbf{r}')=\left(\frac{k_F^\gamma(\mathbf{r})+k_F^\gamma(\mathbf{r}')}{2}\right)^{1/\gamma}, \tag{23}$$

$$k_F(\mathbf{r})=[3\pi^2\rho(\mathbf{r})]^{1/3}, \tag{24}$$

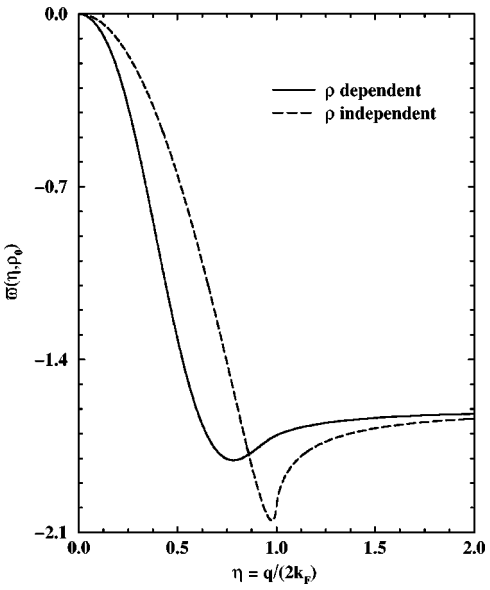

FIG. 1. Kernels in momentum space for the uniform electron gas ρ_0. The KEDF is $T_s^{5/6\pm\sqrt{5}/6}$ for both curves. The broken line is the density-independent kernel; the solid line is the density-dependent kernel with $\gamma=2.7$

where $k_F(\mathbf{r})$ and $\xi_\gamma(\mathbf{r},\mathbf{r}')$ are local one-body and nonlocal two-body Fermi wave vectors, respectively. For the KEDF in Eq. (21) to recover $T_{\rm TF}[\rho]$ at the uniform electron gas limit, the kernel has to be normalized to zero

$$\langle w_{\alpha,\beta}[\xi_\gamma(\mathbf{r},\mathbf{r}'),\mathbf{r}-\mathbf{r}']\rangle=0. \tag{25}$$

The specific choice of the two-body Fermi wave vector $\xi_\gamma(\mathbf{r},\mathbf{r}')$ is based on natural variable arguments;[15] Eq. (22) clearly resembles Eq. (9).

After enforcing the exact LR at the uniform electron gas limit as done in Eq. (10), one obtains the following universal second-order differential equation for every fixed value of q:

$$\eta^2\tilde{w}''_{\alpha,\beta}(\eta,\rho_0)+[\gamma+1-6(\alpha+\beta)]\eta\tilde{w}'_{\alpha,\beta}(\eta,\rho_0) +36\alpha\beta\tilde{w}_{\alpha,\beta}(\eta,\rho_0)=20G(\eta)\rho_0^{5/3-(\alpha+\beta)}, \tag{26}$$

where $\tilde{w}'_{\alpha,\beta}(\eta,\rho_0)$ and $\tilde{w}''_{\alpha,\beta}(\eta,\rho_0)$ are the first and the second derivatives of $\tilde{w}_{\alpha,\beta}(\eta,\rho_0)$ with respect to η, respectively. Note that γ is explicitly involved in the determination of the kernel, and if $\alpha+\beta=\frac{5}{3}$, the term involving ρ_0 on the right-hand side of Eq. (26) disappears. Also note that Eq. (26) is fully consistent with Eq. (16) if the kernel is density-independent, which simply removes the first two terms involving derivatives in the left-hand side of Eq. (26). Solving this universal second-order differential equation is straightforward via standard techniques, such as a power series solution.[18,19] Figure 1 compares one such density-dependent kernel in momentum space for $\{\alpha,\beta\}=\{\frac{5}{6}\pm\sqrt{5}/6\}$ and $\gamma=2.7$ with its density-independent counterpart. Note the sizable effect of the density-dependence on the kernel.

Following the same procedure as given before,[6] one can consider the limits of the new KEDF for $q\to0$ and $q\to\infty$. This involves substituting the exact solution of Eq. (26) into Eq. (22), Fourier transforming the resultant expression, and then grouping terms in various orders of $\delta\sigma$. We obtain, at the $q\to0$ limit,

$$T_s^{\alpha,\beta}\to T_{\rm TF}+(1-a_0)\ T_{\rm vW}-a_0(\alpha+\beta-1)\langle\delta\sigma|t_{\rm vW}\rangle-\frac{a_0}{2}(\alpha+\beta-1)(\alpha+\beta-2)\langle\delta\sigma^2|t_{\rm vW}\rangle+\mathcal{O}(\delta\sigma^3), \tag{27}$$

$$a_0=\frac{32\alpha\beta}{36\alpha\beta-9(\alpha+\beta-1)(\alpha+\beta+1-\gamma/3)}, \tag{28}$$

and at the $q\to\infty$ limit,

$$T_s^{\alpha,\beta}\to T_{\rm vW}+(1-a_\infty)T_{\rm TF}-a_\infty\left(\alpha+\beta-\frac{5}{3}\right)\langle\delta\sigma|t_{\rm TF}\rangle -\frac{a_\infty}{2}\left(\alpha+\beta-\frac{5}{3}\right)\left(\alpha+\beta-\frac{8}{3}\right)\langle\delta\sigma^2|t_{\rm TF}\rangle+\mathcal{O}(\delta\sigma^3), \tag{29}$$

$$a_\infty=\frac{32}{36\alpha\beta-9(\alpha+\beta-5/3)(\alpha+\beta+5/3-\gamma/3)}. \tag{30}$$

One can easily see the differences between Eqs. (17) and (27) and between Eqs. (18) and (29); the density-dependence in the kernel is responsible for the second terms in the denominators in Eqs. (28) and (30). Once again, we find no single set of $\{\alpha,\beta,\gamma\}$ that simultaneously removes all spurious $\delta\sigma$ terms in Eqs. (27) and (29) and makes them reduce to the second-order CGE and the CLQL, respectively. However, the set $\{\alpha,\beta\}=\{5/6\pm\sqrt{5}/6\}$ is particularly attractive because it forces Eq. (29) to yield the CLQL, which is more important than the $q\to0$ limit (the second-order CGE).[6] We can then use the third parameter γ to fine-tune the behavior around the $q\to0$ limit so that the effect of the spurious $\delta\sigma$ terms and the leading terms in Eq. (27) can be well balanced. Of course, for this given set of $\{\alpha,\beta\}$, enforcing the second-order CGE can provide a value for γ, but the effect of these spurious $\delta\sigma$ terms then cannot be simply controlled. This will be discussed further in Sec. V.

IV. NUMERICAL IMPLEMENTATIONS

A. Hohenberg-Kohn self-consistent optimization

The Hohenberg-Kohn[20] (HK) total energy functional in terms of $\rho(\mathbf{r})$ is written as

$$E_{\rm tot}[\rho]=T_s[\rho]+V_{ne}[\rho]+J[\rho]+E_{xc}[\rho]+V_{nn}, \tag{31}$$

where V_{ne}, J, E_{xc}, and V_{nn} are the electron-nuclear attraction (including pseudopotentials), electron-electron Coulomb repulsion, electron exchange-correlation, and nuclear-nuclear Coulomb repulsion energy functionals, respectively. For a system with a fixed number of electrons N, one can write down the functional $\Pi[\rho]$:

$$\Pi[\rho]=E_{\rm tot}[\rho]-\mu\langle\rho(\mathbf{r})\rangle, \tag{32}$$

where μ is the Lagrange multiplier. To determine the ground-state of the system, $\Pi[\rho]$ must be minimized with respect to $\rho(\mathbf{r})$. However, during the minimization process, it is absolutely necessary to maintain the positivity of $\rho(\mathbf{r})$. This is not guaranteed in general if $\rho(\mathbf{r})$ is used as the generalized coordinate in conventional optimization algorithms[19] such as the steepest-descent or conjugate-gradient methods. To circumvent this problem, one can work with a new variable $\varphi(\mathbf{r})$

$$\rho(\mathbf{r})=\varphi^2(\mathbf{r}), \tag{33}$$

which ensures a positive $\rho(\mathbf{r})$ during the entire minimization.

Based on a first-order differential equation with a fictitious time τ

$$\frac{d\varphi(\mathbf{r})}{d\tau}+\frac{\delta\Pi}{\delta\varphi(\mathbf{r})}=0, \tag{34}$$

the steepest-descent approach is the simplest scheme[2]

$$\varphi_{n+1}(\mathbf{r})=\varphi_n(\mathbf{r})-\Delta\frac{\delta\Pi}{\delta\varphi_n(\mathbf{r})}, \tag{35}$$

$$\frac{\delta\Pi}{\delta\varphi_n(\mathbf{r})}=\frac{\delta\Pi}{\delta\rho_n(\mathbf{r})}\frac{\delta\rho_n(\mathbf{r})}{\delta\varphi_n(\mathbf{r})}=2\varphi_n(\mathbf{r})\left(\frac{\delta E_{\rm tot}}{\delta\rho_n(\mathbf{r})}-\mu\right), \tag{36}$$

where Δ is the step size and $\delta\Pi/\delta\varphi_n(\mathbf{r})$ is the steepest-descent vector at the nth iteration. In this work, we have formulated the energy minimization in terms of a damped second-order equation of motion[21] for the generalized coordinate $\varphi(\mathbf{r})$

$$\frac{d^2\varphi(\mathbf{r})}{d\tau^2}+\zeta\frac{d\varphi(\mathbf{r})}{d\tau}+\frac{\delta\Pi}{\delta\varphi(\mathbf{r})}=0, \tag{37}$$

which yields

$$\varphi_{n+1}(\mathbf{r})=(1+\Omega)\varphi_n(\mathbf{r})-\Omega\varphi_{n-1}(\mathbf{r})-\Omega\Delta^2\frac{\delta\Pi}{\delta\varphi_n(\mathbf{r})}, \tag{38}$$

$$\Omega=\frac{1}{1+\zeta\Delta}. \tag{39}$$

Here ζ is a damping or friction coefficient. We have found that this scheme is not only easy to implement, but also offers greater stability even when Δ becomes much larger than that of the simple steepest-descent method. We have also found that minimization algorithms based on the conjugate-gradient method actually converge faster, but require very accurate line minimizations that can be difficult to implement. The Lagrange multiplier μ is determined dynamically by multiplying both sides of Eq. (38) by $\varphi_n(\mathbf{r})$ and integrating over all space:

$$\mu=\frac{\langle\varphi_n|\varphi_{n+1}\rangle-(1+\Omega)\langle\varphi_n|\varphi_n\rangle+\Omega\langle\varphi_n|\varphi_{n-1}\rangle+2\Omega\Delta^2\langle\varphi_n|\,\delta E_{\rm tot}/\delta\rho_n|\varphi_n\rangle}{2\langle\varphi_n|\varphi_n\rangle}. \tag{40}$$

Conventional plane-wave-basis techniques[22,23] were used to set up the various potential terms in the self-consistent Thomas-Fermi-like equation[10,13,20]

$$\frac{\delta E_{\rm tot}[\rho]}{\delta\rho(\mathbf{r})}=\mu. \tag{41}$$

Note that since this scheme is purely based on $\rho(\mathbf{r})$, only local pseudopotentials[24,25] can be used to calculate the V_{ne} term.

B. Evaluation of the density-dependent kernel

The presence of density-dependent terms inside the kernels in Eq. (21) makes a straightforward application of a fast Fourier transform (FFT) impossible. However, one can use a Taylor series expansion[18] to factor out the density-dependence in the kernel. For example, the double-density-dependent kernel in real space can be written as (up to second order),

$$\begin{aligned}w_{\alpha,\beta}[\xi_\gamma(\mathbf{r},\mathbf{r}'),\mathbf{r}-\mathbf{r}']=&\,w_{\alpha,\beta}(k_F^*,\mathbf{r}-\mathbf{r}')+\left.\frac{\partial w_{\alpha,\beta}[\xi_\gamma(\mathbf{r},\mathbf{r}'),\mathbf{r}-\mathbf{r}']}{\partial\rho(\mathbf{r})}\right|_{\rho_*}\theta(\mathbf{r})+\left.\frac{\partial w_{\alpha,\beta}[\xi_\gamma(\mathbf{r},\mathbf{r}'),\mathbf{r}-\mathbf{r}']}{\partial\rho(\mathbf{r}')}\right|_{\rho_*}\theta(\mathbf{r}')\\&+\frac{\partial^2 w_{\alpha,\beta}[\xi_\gamma(\mathbf{r},\mathbf{r}'),\mathbf{r}-\mathbf{r}']}{\partial\rho^2(\mathbf{r})}_{\rho_*}\frac{\theta^2(\mathbf{r})}{2}+\left.\frac{\partial^2 w_{\alpha,\beta}[\xi_\gamma(\mathbf{r},\mathbf{r}'),\mathbf{r}-\mathbf{r}']}{\partial\rho^2(\mathbf{r}')}\right|_{\rho_*}\frac{\theta^2(\mathbf{r}')}{2}\\&+\frac{\partial^2 w_{\alpha,\beta}[\xi_\gamma(\mathbf{r},\mathbf{r}'),\mathbf{r}-\mathbf{r}']}{\partial\rho(\mathbf{r})\partial\rho(\mathbf{r}')}_{\rho_*}\theta(\mathbf{r})\theta(\mathbf{r}')+\cdots,\end{aligned} \tag{42}$$

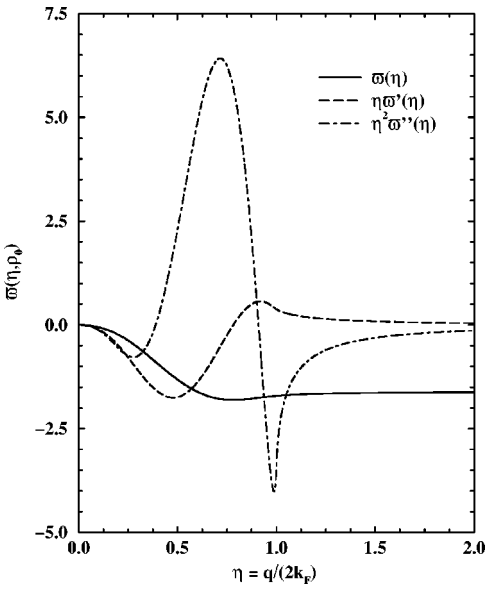

FIG. 2. Double-density-dependent kernel and its derivatives in momentum space for the uniform electron gas ρ_0. The KEDF is $T_s^{5/6\pm\sqrt{5}/6}$ with $\gamma=2.7$.

where $\theta(\mathbf{r})=\rho(\mathbf{r})-\rho_*$, and $k_F^*=(3\pi^2\rho_*)^{1/3}$ are the deviation from, and Fermi wave vector magnitude of, a reference uniform density ρ_*. It is clear that the density-dependence is absorbed into simple powers of $\theta(\mathbf{r})$, and that all the partial differentials are functions of ρ_*, which can be evaluated via an FFT

$$\hat{F}\left(\left.\frac{\partial w_{\alpha,\beta}[\xi_\gamma(\mathbf{r},\mathbf{r}'),\mathbf{r}-\mathbf{r}']}{\partial\rho(\mathbf{r})}\right|_{\rho_*}\right)=-\frac{\eta_*\tilde{w}'_{\alpha,\beta}(\eta_*,\rho_*)}{6\rho_*}, \tag{43}$$

$$\hat{F}\left(\left.\frac{\partial^2 w_{\alpha,\beta}[\xi_\gamma(\mathbf{r},\mathbf{r}'),\mathbf{r}-\mathbf{r}']}{\partial\rho^2(\mathbf{r})}\right|_{\rho_*}\right)=\frac{\eta_*^2\tilde{w}''_{\alpha,\beta}(\eta_*,\rho_*)+(7-\gamma)\eta_*\tilde{w}'_{\alpha,\beta}(\eta_*,\rho_*)}{36\rho_*^2}, \tag{44}$$

$$\hat{F}\left(\left.\frac{\partial^2 w_{\alpha,\beta}[\xi_\gamma(\mathbf{r},\mathbf{r}'),\mathbf{r}-\mathbf{r}']}{\partial\rho(\mathbf{r})\partial\rho(\mathbf{r}')}\right|_{\rho_*}\right)=\frac{\eta_*^2\tilde{w}''_{\alpha,\beta}(\eta_*,\rho_*)+(1+\gamma)\eta_*\tilde{w}'_{\alpha,\beta}(\eta_*,\rho_*)}{36\rho_*^2}, \tag{45}$$

where $\eta_*=q/(2k_F^*)$, and $\tilde{w}'_{\alpha,\beta}(\eta_*,\rho_*)$ and $\tilde{w}''_{\alpha,\beta}(\eta_*,\rho_*)$ are the first and the second derivatives of $\tilde{w}_{\alpha,\beta}(\eta_*,\rho_*)$ with respect to η_*, respectively. Figure 2 shows one such kernel and its derivatives in momentum space for $\{\alpha,\beta\}=\{\frac{5}{6}\pm\sqrt{5}/6\}$ and $\gamma=2.7$.

For maximum numerical efficiency, all derivative terms of the kernel are kept in momentum space so that one FFT is saved for each of their evaluations. For example, during the evaluation of Eq. (15), the first FFT can be avoided:

$$\begin{aligned}T_Y^{\alpha,\beta}[\rho]&=C_{\mathrm{TF}}\langle\rho^\alpha(\mathbf{r})|w_{\alpha,\beta}(\mathbf{r}-\mathbf{r}')|\rho^\beta(\mathbf{r}')\rangle\\&=\frac{C_{\mathrm{TF}}}{V}\sum_{\mathbf{q}}\tilde{w}_{\alpha,\beta}(\mathbf{q})\langle\rho^\alpha(\mathbf{r})|e^{-i\mathbf{q}\cdot(\mathbf{r}-\mathbf{r}')}|\rho^\beta(\mathbf{r}')\rangle\\&=\frac{C_{\mathrm{TF}}}{V}\sum_{\mathbf{q}}\tilde{w}_{\alpha,\beta}(\mathbf{q})\langle\rho^\alpha(\mathbf{r})e^{-i\mathbf{q}\cdot\mathbf{r}}\rangle\langle\rho^\beta(\mathbf{r})e^{i\mathbf{q}\cdot\mathbf{r}}\rangle\\&=\frac{C_{\mathrm{TF}}}{V}\sum_{\mathbf{q}}\tilde{w}_{\alpha,\beta}(\mathbf{q})\tilde{\rho}_\alpha(-\mathbf{q})\tilde{\rho}_\beta(\mathbf{q}),\end{aligned} \tag{46}$$

where V is the volume of the simulation cell. Now, the computational cost has been reduced from scaling quadratically with grid size[8] to scaling essentially linearly with the system size $\mathcal{O}(N\ln N)$. The current scheme is only three times as expensive as the conventional one based on the density-independent kernel and linear-response theory.[3–6] By contrast, the KEDF's based on quadratic-response theory[3,7] are over ten times as expensive as the KEDF's based on linear-response theory with density-independent kernels.[3–6]

For bulk solids, the natural choice for ρ_* is obviously ρ_0. However, this scheme is only valid for the nearly free electron gas, where $\rho(\mathbf{r})$ does not differ too much from ρ_0. For other systems such as atoms, molecules, and surfaces, this scheme might suffer severely because ρ_0 is no longer well-defined and $\rho(\mathbf{r})$ can have large oscillations and decays to zero asymptotically. On the other hand, if ρ_* is carefully chosen to treat high-density regions satisfactorily, the breakdown in those regions where $\rho(\mathbf{r})$ is small and far below ρ_* might not be so severe because the error made in the second-order Taylor series expansion of Eq. (42) might be suppressed by the smallness of $\rho(\mathbf{r})$ in these regions. In the next section, we will show how this can be achieved even for realistic surfaces.

TABLE I. Calculated lattice parameters (Å) for bulk aluminum, compared with Kohn-Sham calculation results. sc stands for simple cubic and dia for diamond. Lattice parameters refer to cell size in cubic unit cells: fcc cell, 4 atoms, bcc cell, 2 atoms; sc cell, 4 atoms; dia cell, 8 atoms.

Model [a]	fcc	bcc	sc	dia
Kohn-Sham	4.03	3.23	5.33	5.84
ρ independent				
$\{\frac{5}{6}\pm 0\}$	4.04	3.23	5.33	5.94
$\{\frac{5}{6}\pm(4\sqrt{2}-5/6)\}$	4.04	3.23	5.33	5.94
$\{\frac{5}{6}\pm\frac{1}{6}\}$	4.04	3.23	5.33	5.95
$\{\frac{5}{6}\pm\frac{1}{3}\}$	4.04	3.23	5.33	5.97
$\{\frac{5}{6}\pm\sqrt{5}/6\}$	4.03	3.23	5.33	5.97
ρ dependent				
$\{\frac{5}{6}\pm 0\}_{1.9}$	4.04	3.22	5.37	5.92
$\{\frac{5}{6}\pm(4\sqrt{2}-5/6)\}_{2.0}$	4.04	3.22	5.37	5.92
$\{\frac{5}{6}\pm\frac{1}{6}\}_{2.1}$	4.03	3.22	5.37	5.92
$\{\frac{5}{6}\pm\frac{1}{3}\}_{2.5}$	4.03	3.22	5.37	5.92
$\{\frac{5}{6}\pm\sqrt{5}/6\}_{2.7}$	4.03	3.22	5.38	5.92

[a]For the ρ independent, $\{\alpha,\beta\}$ is shown; for the ρ dependent, $\{\alpha,\beta\}_\gamma$ is shown.

TABLE II. Calculated energy per atom (eV) for bulk aluminum, compared with Kohn-Sham calculation results. The last two columns are the vacancy formation (vf) energies, the first column is the energy for the fcc structure, while other columns are energy deviations from the fcc structure. sc stands for simple cubic and dia for diamond.

Model [a]	fcc	hcp [b]	bcc	sc	dia	vf4 [c]	vf32 [c]
Kohn-Sham	−58.336	0.060	0.068	0.250	0.599	0.646	0.626
ρ independent							
$\{\frac{5}{6}\pm 0\}$	−58.331	0.050	0.060	0.227	0.673	1.104	1.371
$\{\frac{5}{6}\pm(4\sqrt{2}-5/6)\}$	−58.331	0.050	0.061	0.226	0.669	1.101	1.369
$\{\frac{5}{6}\pm\frac{1}{6}\}$	−58.331	0.050	0.061	0.226	0.664	1.100	1.363
$\{\frac{5}{6}\pm\frac{1}{3}\}$	−58.333	0.050	0.061	0.221	0.636	1.079	1.346
$\{\frac{5}{6}\pm\sqrt{5}/6\}$	−58.334	0.050	0.061	0.219	0.626	1.077	1.350
ρ dependent							
$\{\frac{5}{6}\pm 0\}_{1.9}$	−58.328	0.058	0.065	0.225	0.592	0.693	0.610
$\{\frac{5}{6}\pm(4\sqrt{2}-5/6)\}_{2.0}$	−58.328	0.058	0.067	0.224	0.595	0.693	0.620
$\{\frac{5}{6}\pm\frac{1}{6}\}_{2.1}$	−58.328	0.058	0.065	0.224	0.596	0.689	0.624
$\{\frac{5}{6}\pm\frac{1}{3}\}_{2.5}$	−58.331	0.058	0.066	0.219	0.585	0.658	0.614
$\{\frac{5}{6}\pm\sqrt{5}/6\}_{2.7}$	−58.331	0.058	0.066	0.217	0.584	0.650	0.628

[a]For the ρ independent, $\{\alpha,\beta\}$ is shown; for the ρ dependent, $\{\alpha,\beta\}_\gamma$ is shown.

[b]The hcp calculations were performed using the fcc nearest neighbor distance for each case. Four atoms were set up in an orthogonal system in the ratio $a:b:c=1:\sqrt{3}:\sqrt{8/3}$.

[c]vf4 is for four-site simulation cell (3 atoms + 1 vacancy); vf32 is for 32-site simulation cell (31 atoms + 1 vacancy). The experimental vf number is 0.66 eV (Ref. 32).

V. RESULTS AND DISCUSSION

After the publication of our previous paper,[6] we found that the real-space evaluation of $\nabla\rho(\mathbf{r})$ (needed for the evaluation of $T_{\mathrm{vW}}[\rho]$) was strongly affected by the fineness of the mesh chosen for a given simulation cell, the plane-wave cutoff (400 eV) used for the Goodwin-Needs-Heine local pseudopotential for aluminum[25] was not sufficient, and the Kohn-Sham (KS) calculations[26] (used for comparison with the HK orbital-free calculations) had not been fully converged with respect to the **k**-point sampling.[9] To remedy the first problem, we now evaluate $\nabla\rho(\mathbf{r})$ in momentum space.[27] This scheme is very stable (up to 0.001 eV) against changes of the mesh beyond a certain minimum mesh size. We also increased the plane-wave cutoff to 600 eV, and converged the KS calculations with respect to the **k**-point sampling.[9] The KS calculations were performed using the plane-wave DFT code CASTEP (Ref. 23) with the finest **k**-point sampling allowed by the code. The exchange-correlation effects were treated at the local-density approximation level.[28] The corrections to our previous paper[6] will be published as an erratum.[29]

As before, the hcp structure is included in the comparison, since its energy is only slightly above the more stable fcc structure and slightly below the less stable bcc structure, making it an excellent test case for our trial KEDF's. The experimentally well-characterized vacancy formation (vf) energy[30] was also computed to further assess the quality of the trial KEDF's. The vf energy was calculated using both a four-site cell (3 atoms + 1 vacancy) and a 32-site cell (31 atoms + 1 vacancy) via the expression[31]

$$E_{\mathrm{vf}}=E\left(N-1,1,\frac{N-1}{N}V\right)-\frac{N-1}{N}E(N,0,V), \qquad (47)$$

where $E(N,n,V)$ is the energy of the system of N atoms and n vacancies occupying $(N+n)$ sites in a volume V. As the change in the vf energy due to ionic relaxation is minimal,[31] we kept the lattice fixed. Since our plane-wave cutoff and **k**-point sampling are converged further than previous reports,[31] we will use our KS vf numbers as the benchmark.

Tables I and II demonstrate that the inclusion of the density-dependence in the kernel improves the performance of KEDF's. We do not include other KEDF's whose $\alpha+\beta\neq\frac{5}{3}$, because of their poor performance. For KEDF's with density-dependent kernels, only those with the optimal γ values (up to the second decimal point) are shown. As discussed in Sec. III, only $T_s^{5/6\pm\sqrt{5}/6}$ satisfies the $q\to\infty$ limit; all others shown in Tables I and II display the delicate interplay between the effects of the fulfillment of the $q\to\infty$ and $q\to 0$ limits and the elimination of those spurious $\delta\sigma$ terms. The specific choices of other $\{\alpha,\beta\}$ are mainly for comparison purposes, except for the one suggested by Wang and Teter,[3] $\{\alpha,\beta\}=\{\frac{5}{6}\pm(4\sqrt{2}-5)/6\}$. Without the density-dependence in the kernel, the KEDF's do not even approach the KS vf energies, since the order-of-magnitude change in $\rho(\mathbf{r})$ in the vacancy region is most certainly not nearly-free-electron-like. However, after the inclusion of the density-dependence in the kernel, the KEDF's show significant improvement, especially for the vf energies, if the free parameter γ is carefully tuned. Note also the tiny gaps between the fcc, hcp, and bcc structures are faithfully reproduced, and even the absolute total energies are very close to the KS results. At a finer scale, $T_s^{5/6\pm\sqrt{5}/6}$ with $\gamma=2.7$ stands out clearly as the best KEDF; any deviation from $\{\alpha,\beta\}=\{\frac{5}{6}\pm\sqrt{5}/6\}$, however small, degrades the performance.

The next logical step is testing our new KEDF's on sys-

TABLE III. Calculated surface energy (mJ/m^2) for aluminum low-index fcc surfaces, compared with Kohn-Sham calculation results. The vacuum has the same thickness as the slab. The fcc-(110) slab has seven layers of atoms, and both of the fcc-(100) and the fcc-(111) slabs have five layers of atoms, respectively.

Model [a]	(110)	(100)	(111)
Kohn-Sham	986	889	820
ρ independent			
$\{\frac{5}{6}\pm 0\}$	1910	1921	1775
$\{\frac{5}{6}\pm(4\sqrt{2}-5/6)\}$	1907	1919	1773
$\{\frac{5}{6}\pm\frac{1}{6}\}$	1902	1915	1769
$\{\frac{5}{6}\pm\frac{1}{3}\}$	1877	1894	1751
$\{\frac{5}{6}\pm\sqrt{5}/6\}$	1868	1887	1744
ρ dependent			
$\{\frac{5}{6}\pm 0\}_{1.9}$	1203	1183	1001
$\{\frac{5}{6}\pm(4\sqrt{2}-5/6)\}_{2.0}$	1205	1186	1008
$\{\frac{5}{6}\pm\frac{1}{6}\}_{2.1}$	1196	1178	1000
$\{\frac{5}{6}\pm\frac{1}{3}\}_{2.5}$	1074	1060	876
$\{\frac{5}{6}\pm\sqrt{5}/6\}_{2.7}$	1053	1043	857

[a]For the ρ independent, $\{\alpha,\beta\}$ is shown; for the ρ dependent, $\{\alpha,\beta\}_\gamma$ is shown.

tems with even more drastic density changes, e.g., realistic surfaces. Those KEDF's without the density-dependence in the kernel can be readily applied to such systems without any numerical instability. However, Table III reveals that for the same group of KEDF's with density-independent kernels, the surface energies are off by a factor of 2 compared with KS predictions and the (110)–(100) ordering is reversed. A more troublesome finding is that the surface energy strongly depends on the size of the vacuum, which directly dictates the value for the average surface density, $\rho_0^{\rm surf}$. This is certainly

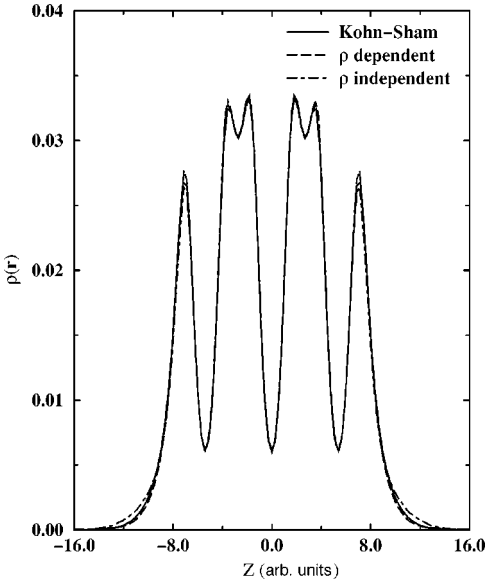

FIG. 4. Density cross section for aluminum fcc-(110) surface. The KEDF is $T_s^{5/6\pm\sqrt{5}/6}$ for both nonsolid curves. The long-dashed line is for the density-dependent kernel with $\gamma=2.7$; the dot-dashed line is for the density-independent kernel. $\rho_*=\rho_0^{\rm bulk}$.

a highly undesirable feature. However, Figs. 3–5 clearly show that $\rho(\mathbf{r})$ obtained from the solution of the self-consistent Thomas-Fermi-like equation,[10,13,20] Eq. (41), closely matches the KS $\rho(\mathbf{r})$ for every case of the aluminum low-index fcc surfaces (100), (110), and (111). This suggests that the kinetic-energy potentials, $\delta T_s[\rho]/\delta\rho(\mathbf{r})$, of the simpler KEDF's based on a density-independent kernel are of high quality. This further supports the utility of such KEDF's in the recently proposed embedding formalism[32] that uses $\delta T_s[\rho]/\delta\rho(\mathbf{r})$.

Unfortunately, with the vacuum-size-dependent $\rho_0^{\rm surf}$ as ρ_*, a straightforward application of those KEDF's with the

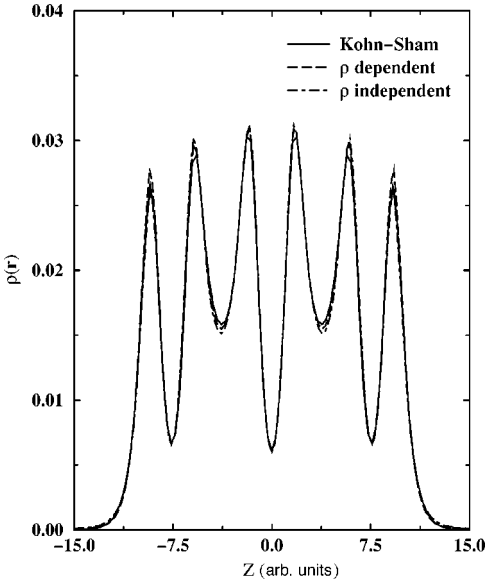

FIG. 3. Density cross section for aluminum fcc-(100) surface. The KEDF is $T_s^{5/6\pm\sqrt{5}/6}$ for both nonsolid curves. The long-dashed line is for the density-dependent kernel with $\gamma=2.7$; the dot-dashed line is for the density-independent kernel. $\rho_*=\rho_0^{\rm bulk}$.

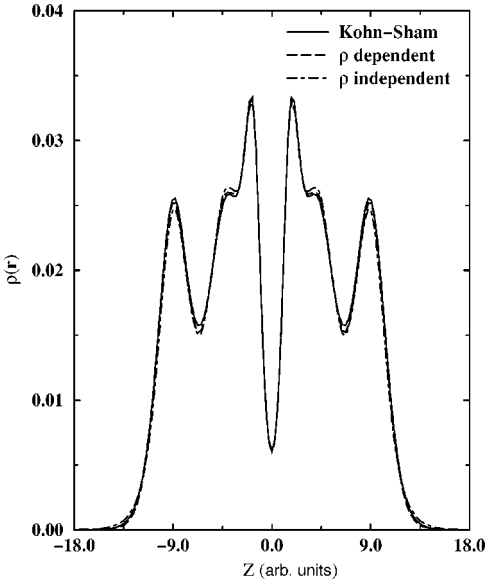

FIG. 5. Density cross section for aluminum fcc-(111) surface. The KEDF is $T_s^{5/6\pm\sqrt{5}/6}$ for both nonsolid curves. The long-dashed line is for the density-dependent kernel with $\gamma=2.7$; the dot-dashed line is for the density-independent kernel. $\rho_*=\rho_0^{\rm bulk}$.

TABLE IV. Contributions of different orders in the Taylor series expansion of the kernel, Eq. (42), to the surface energy (mJ/m^2) for aluminum low-index fcc surfaces. The KEDF is $T_s^{5/6\pm\sqrt{5}/6}$ with $\gamma=2.7$.

Surface	0th	1st	2nd	Total
(110)	561	484	8	1053
(100)	671	386	−14	1043
(111)	395	446	16	857

density-dependent kernels refuses to converge because the second-order Taylor series expansion in Eq. (42) makes too big an error in regions where $\rho(\mathbf{r})$ is large. To our surprise, we found that if ρ_* is chosen to be the bulk-phase average density ρ_0^{bulk}, the KEDF's with the density-dependent kernels not only converge properly, but also bring the surface energies much closer to the KS results (Table III), including reproducing the correct ordering of the surface stabilities. Figures 3–5 also depict some non-trivial improvements in the density profiles. This surprising success stems from the smallness of the fast-decaying density outside the surface slab, which actually suppresses the error made in the finite Taylor series expansion in Eq. (42).

It is also intriguing to see relative contributions of different orders in the Taylor series expansion of the kernel, Eq. (42), to the surface energy. Table IV shows that zeroth and first orders contribute most while second order only accounts for less than 2% of the total surface energy. This is a clear sign of convergence of the second-order Taylor series expansion, even for large density variations.

Of course, there is still room for further improvement. It remains to be seen whether the free parameter γ is system-independent. More applications and tests are surely necessary. Ideally, one would like to remove ρ_* from the construction of the KEDF completely, but maintaining the $\mathcal{O}(N \ln N)$ scaling may then be impossible. More likely, one would end up with a method with $\mathcal{O}(N^2)$ scaling, as Chacón and co-workers have developed.[8] An $\mathcal{O}(N \ln N)$ method without ρ_0 in the construction is under development at this time; the details of which will be reported later.[33]

VI. CONCLUSION

In conclusion, we have devised a family of kinetic-energy density functionals which further generalize and improve upon the Wang-Teter, Perrot, Smargiassi-Madden, and Wang-Govind-Carter kinetic-energy density functionals.[3–7] These functionals are still based on linear-response theory. The simple, effective implementation scheme for the nearly free electron gas delivers $\mathcal{O}(N \ln N)$ scaling even for the double-density-dependent kernel. Numerical tests show that, compared with those kinetic-energy density functionals based on quadratic-response theory,[3,7] our functionals can yield similar results for bulk solids, but with a lower computational cost and simpler implementation. More interestingly, all KEDF's regardless of their kernels' density dependence are seen to have very high-quality $\delta T_s[\rho]/\delta\rho(\mathbf{r})$, even for large density variations as at realistic surfaces. This lends credence to their use in the recently developed embedding method that offers a systematic means of improving upon the Kohn-Sham description[13,26] in a local region.[32] In addition, we have shown how the surface energy can be greatly improved by a simple, yet reasonable choice of average density. Finally, utilizing our functionals in $\mathcal{O}(N \ln N)$ methods of first-principles molecular dynamics[2,5,7] has a promising future.

ACKNOWLEDGMENTS

We thank Dr. Stuart C. Watson for his help in calibrating our code and for his constructive comments on this manuscript. We thank Professor Paul A. Madden for helpful discussions. Financial support for this project was provided by the National Science Foundation, the Army Research Office, and the Air Force Office of Scientific Research.

[1] O. F. Sankey and D. J. Niklewski, Phys. Rev. B **40**, 3979 (1989); W. Yang, Phys. Rev. Lett. **66**, 1438 (1991); G. Galli and M. Parrinello, *ibid.* **69**, 3547 (1992); S. Baroni and P. Giannozzi, Europhys. Lett. **17**, 547 (1992); W. Kohn, Chem. Phys. Lett. **208**, 167 (1993); F. Mauri, G. Galli, and R. Car, Phys. Rev. B **47**, 9973 (1993); X. P. Li, W. Nunes, and D. Vanderbilt, *ibid.* **47**, 10 891 (1993); M. S. Daw, *ibid.* **47**, 10 895 (1993); P. Ordejón, D. A. Drabold, M. P. Grumbach, and R. M. Martin, *ibid.* **48**, 14 646 (1993); P. Ordejón, D. A. Drabold, R. M. Martin, and M. P. Grumbach, *ibid.* **51**, 1456 (1995); E. B. Stechel, A. R. Williams, and P. J. Feibelman, *ibid.* **49**, 10 088 (1994); W. Hierse and E. B. Stechel, *ibid.* **50**, 17 811 (1994); W. Kohn, Phys. Rev. Lett. **76**, 3168 (1996).

[2] N. Govind, J. Wang, and H. Guo, Phys. Rev. B **50**, 11 175 (1994); N. Govind, J. L. Mozos, and H. Guo, *ibid.* **51**, 7101 (1995); D. Nehete, V. Shah, and D. G. Kanhere, *ibid.* **53**, 2126 (1996); V. Shah, D. Nehete, and D. G. Kanhere, J. Phys.: Condens. Matter **6**, 10 773 (1994); V. Shah, D. G. Kanhere, C. Majumder, and D. G. Das, *ibid.* **9**, 2165 (1997).

[3] L.-W. Wang and M. P. Teter, Phys. Rev. B **45**, 13 196 (1992).

[4] F. Perrot, J. Phys.: Condens. Matter **6**, 431 (1994); M. Pearson, E. Smargiassi, and P. A. Madden, *ibid.* **5**, 3321 (1993).

[5] E. Smargiassi and P. A. Madden, Phys. Rev. B **49**, 5220 (1994); E. Smargiassi and P. A. Madden, *ibid.* **51**, 117 (1995); M. Foley, E. Smargiassi, and P. A. Madden, J. Phys.: Condens. Matter **6**, 5231 (1994).

[6] Y. A. Wang, N. Govind, and E. A. Carter, Phys. Rev. B **58**, 13 465 (1998).

[7] M. Foley and P. A. Madden, Phys. Rev. B **53**, 10 589 (1996); B. J. Jesson, M. Foley, and P. A. Madden, *ibid.* **55**, 4941 (1997).

[8] E. Chacón, J. E. Alvarellos, and P. Tarazona, Phys. Rev. B **32**, 7868 (1985); P. García-González, J. E. Alvarellos, and E. Chacón, *ibid.* **53**, 9509 (1996); P. García-González, J. E. Alvarellos, and E. Chacón, *ibid.* **57**, 4857 (1998); P. García-González, J. E. Alvarellos, and E. Chacón, Phys. Rev. A **54**, 1897 (1996); P. García-González, J. E. Alvarellos, and E. Chacón, *ibid.* **57**, 4192 (1998).

[9] A. Baldereschi, Phys. Rev. B **7**, 5215 (1973); D. J. Chadi and M.

L. Cohen, *ibid.* **8**, 5747 (1973); H. J. Monkhorst and J. D. Pack, *ibid.* **13**, 5188 (1976); R. A. Evarestov and V. P. Smirnov, Phys. Status Solidi B **119**, 9 (1983).

[10] L. H. Thomas, Proc. Cambridge Philos. Soc. **23**, 542 (1927); E. Fermi, Rend. Accad., Lincei **6**, 602 (1927); E. Fermi, Z. Phys. **48**, 73 (1928).

[11] C. F. von Weizsäcker, Z. Phys. **96**, 431 (1935).

[12] Z.-Z. Yang, S. Liu, and Y. A. Wang, Chem. Phys. Lett. **258**, 30 (1996).

[13] For example, R. G. Parr and W. Yang, *Density-Functional Theory of Atoms and Molecules* (Oxford University Press, New York, 1989); R. M. Dreizler and E. K. U. Gross, *Density Functional Theory: An Approach to the Quantum Many-Body Problem* (Springer-Verlag, Berlin, 1990).

[14] For example, E. R. Davidson, *Reduced Density Matrices in Quantum Chemistry* (Academic, New York, 1976).

[15] Y. A. Wang, Phys. Rev. A **55**, 4589 (1997).

[16] For example, D. G. Pettifor, *Bonding and Structure of Molecules and Solids* (Clarendon Press, Oxford, 1995); N. W. Ashcroft and N. D. Mermin, *Solid State Physics* (Holt Rinehart & Winston, Philadelphia, 1976); W. A. Harrison, *Solid State Theory* (Dover, New York, 1980); J. Lindhard, K. Dan. Vidensk. Selsk. Mat. Fys. Medd. **28**, 8 (1954).

[17] D. A. Kirzhnits, Zh. Éksp. Teor. Fiz. **32**, 115 (1957) [Sov. Phys. JETP **5**, 64 (1957)]; C. H. Hodges, Can. J. Phys. **51**, 1428 (1973); M. Brack, B. K. Jennings, and Y. H. Chu, Phys. Lett. **65B**, 1 (1976); B. Grammaticos and A. Voros, Ann. Phys. (N.Y.) **123**, 359 (1979); D. R. Murphy, Phys. Rev. A **24**, 1682 (1981).

[18] For example, G. B. Arfken and H. J. Weber, *Mathematical Methods for Physicists*, 4th ed. (Academic, San Diego, California, 1995).

[19] W. H. Press, S. A. Teukolsky, W. T. Vetterling, and B. P. Flannery, *Numerical Recipes in Fortran; The Art of Scientific Computing*, 2nd ed. (Cambridge University, New York, 1992).

[20] P. Hohenberg and W. Kohn, Phys. Rev. **136**, B864 (1964).

[21] M. C. Payne, J. D. Joannopoulos, D. C. Allan, M. P. Teter, and D. H. Vanderbilt, Phys. Rev. Lett. **56**, 2656 (1986); F. Tassone, F. Mauri, and R. Car, Phys. Rev. B **50**, 10 561 (1994).

[22] W. E. Pickett, Comput. Phys. Rep. **9**, 115 (1989).

[23] M. C. Payne, M. P. Teter, D. C. Allan, T. A. Arias, and J. D. Joannopoulos, Rev. Mod. Phys. **64**, 1045 (1992).

[24] T. Starkloff and J. D. Joannopoulos, Phys. Rev. B **16**, 5212 (1977).

[25] L. Goodwin, R. J. Needs, and V. Heine, J. Phys.: Condens. Matter **2**, 351 (1990).

[26] W. Kohn and L. J. Sham, Phys. Rev. **140**, A1133 (1965).

[27] J. A. White and D. M. Bird, Phys. Rev. B **50**, 4954 (1994).

[28] D. J. Ceperley and B. J. Alder, Phys. Rev. Lett. **45**, 566 (1980); J. P. Perdew and A. Zunger, Phys. Rev. B **23**, 5048 (1981).

[29] Y. A. Wang, N. Govind, and E. A. Carter, this issue, Phys. Rev. B **60**, 17 162 (1999).

[30] M. Triftshäuser, Phys. Rev. B **12**, 4634 (1975); A. S. Berger, S. T. Ockers, and R. W. Siegel, J. Nucl. Mater. **69&70**, 734 (1978); M. J. Fluss, L. C. Smedskjaer, M. K. Chason, D. G. Legnini, and R. W. Siegel, Phys. Rev. B **17**, 3444 (1978).

[31] M. J. Gillan, J. Phys.: Condens. Matter **1**, 689 (1989).

[32] N. Govind, Y. A. Wang, A. J. R. da Silva, and E. A. Carter, Chem. Phys. Lett. **295**, 129 (1998); N. Govind, Y. A. Wang, and E. A. Carter, J. Chem. Phys. **110**, 7677 (1999).

[33] Y. A. Wang and E. A. Carter (unpublished).

Erratum: Orbital-free kinetic-energy density functionals with a density-dependent kernel [Phys. Rev. B 60, 16 350 (1999)]

Yan Alexander Wang, Niranjan Govind, and Emily A. Carter
(Published 8 August 2001)

DOI: 10.1103/PhysRevB.64.089903 PACS number(s): 71.15.Mb, 31.15.Ew, 99.10.+g

1. Equation (42) should appear as

$$w_{\alpha,\beta}[\xi_\gamma(\mathbf{r},\mathbf{r}'),\mathbf{r}-\mathbf{r}'] = w_{\alpha,\beta}[k_F^*,\mathbf{r}-\mathbf{r}'] + \left.\frac{\partial w_{\alpha,\beta}[\xi_\gamma(\mathbf{r},\mathbf{r}'),\mathbf{r}-\mathbf{r}']}{\partial\rho(\mathbf{r})}\right|_{\rho_*}\theta(\mathbf{r}) + \left.\frac{\partial w_{\alpha,\beta}[\xi_\gamma(\mathbf{r},\mathbf{r}'),\mathbf{r}-\mathbf{r}']}{\partial\rho(\mathbf{r}')}\right|_{\rho_*}\theta(\mathbf{r}')$$
$$+ \left.\frac{\partial^2 w_{\alpha,\beta}[\xi_\gamma(\mathbf{r},\mathbf{r}'),\mathbf{r}-\mathbf{r}']}{\partial\rho^2(\mathbf{r})}\right|_{\rho_*}\frac{\theta^2(\mathbf{r})}{2} + \left.\frac{\partial^2 w_{\alpha,\beta}[\xi_\gamma(\mathbf{r},\mathbf{r}'),\mathbf{r}-\mathbf{r}']}{\partial\rho^2(\mathbf{r}')}\right|_{\rho_*}\frac{\theta^2(\mathbf{r}')}{2}$$
$$+ \left.\frac{\partial^2 w_{\alpha,\beta}[\xi_\gamma(\mathbf{r},\mathbf{r}'),\mathbf{r}-\mathbf{r}']}{\partial\rho(\mathbf{r})\partial\rho(\mathbf{r}')}\right|_{\rho_*}\theta(\mathbf{r})\theta(\mathbf{r}') + \cdots, \tag{42}$$

where all derivative terms should be evaluated at a reference uniform density ρ_*.

2. In the caption of Table I, sc cell has 8 atoms (instead of 4 atoms).

3. In Tables I–III, each occurrence of $\{\frac{5}{6}\pm(4\sqrt{2}-5/6)\}$ should have been printed as $\{\frac{5}{6}\pm(4\sqrt{2}-5)/6\}$.

4. In Figs. 3–5, the units for the x axis should be ''atomic units'' (instead of ''arb. units'').

